Electronic structure of sub-stoichiometric iron aluminide clusters

2001 J. Phys.: Condens. Matter 13 8363

(http://iopscience.iop.org/0953-8984/13/36/310)

INSTITUTE OF PHYSICS PUBLISHING JOURNAL OF PHYSICS: CONDENSED MATTER

J. Phys.: Condens. Matter **13** (2001) 8363–8373 PII: S0953-8984(01)25531-3

Electronic structure of sub-stoichiometric iron aluminide clusters

B V Reddy[1], S C Deevi[1], A C Lilly[2] and P Jena[3]

[1] Research Center, Chrysalis Technologies Incorporated, 7801 White Pine Road, Richmond, VA 23234, USA
[2] Research Development and Engineering Center, Philip Morris, USA, 4201 Commerce Road, Richmond, VA 23234, USA
[3] Department of Physics, Virginia Commonwealth University, Richmond, VA 23284-2000, USA

Received 6 June 2001
Published 23 August 2001
Online at stacks.iop.org/JPhysCM/13/8363

Abstract

The electronic structure of Fe_nAl_m ($n + m = 15$) clusters mimicking $Fe_{1-x}Al_x$ alloys in the $0 < x < 0.5$ composition range is investigated systematically by modelling the system with a 15-atom cluster having a body-centred cubic structure. The calculations are carried out using density-functional theory and the generalized gradient approximation for the exchange-correlation potential. The preferred location of Al atoms as well as the atomic relaxations following Al substitution are determined by minimizing the total energy of the cluster subject to certain symmetry constraints. The electronic energy levels near the Fermi energy are found to be dominated by Fe 3d orbitals for $x < 0.33$. For higher aluminium concentrations, the density of states for the highest occupied molecular orbitals (HOMOs) and lowest unoccupied molecular orbitals (LUMOs) are a strong admixture of Fe 3d and Al 3p orbitals. The filling of the minority spin states of Fe 3d followed by the shifting of the Fermi energy towards Al 3p with successive doping of Al is consistent with the observed anomaly in the electrical resistivity of iron aluminides. This change in the electronic structure is also found to have a significant impact on the magnetic properties of these systems. While the magnetic moment at the individual Fe sites decreases from 3 μ_B to 2 μ_B with increasing Al concentration, the net magnetization undergoes substantial reduction not only because of decreasing Fe content but also because of anti-ferromagnetic coupling between Fe and Al sites. The ability of a finite size cluster to model bulk behaviour is examined.

1. Introduction

Transition metal aluminides in general and iron aluminides in particular have been a subject of great interest for many years. Their excellent oxidation and corrosion resistance properties,

high melting point, low density and low material cost make them ideal candidates for numerous applications [1–4]. Iron aluminides can be formed over the entire composition range ($Fe_{1-x}Al_x$, $0 \leqslant x \leqslant 1$). These have two ordered phases with cubic structures. Fe_3Al has DO_3 crystal structure and is ferromagnetic where two different Fe atoms (Fe_I with eight Fe nearest neighbours, and Fe_{II} with four Fe nearest neighbours) carry different magnetic moments. FeAl, on the other hand, has a B2 crystal structure (CsCl) and is non-magnetic. In addition, Fe–Al alloys in the iron-rich phase remain ferromagnetic while they are nonmagnetic in the aluminium-rich phase. Although a considerable amount of work has been done on the mechanical properties [1–4] of iron aluminides, both experimental and theoretical efforts in understanding the electronic structure of these alloys in the sub-stoichiometric composition are lacking.

Recently, Lilly *et al* [5] have studied electrical resistivity of the $Fe_{1-x}Al_x$ alloy in the ordered B2 phase at room temperature as a function of aluminium content, x. For $0 < x < 0.33$, the resistivity was found to increase with Al concentration while for $x > 0.33$, the resistivity decreases with increasing aluminium concentration. This negative resistivity slope was explained by Lilly *et al* [5] by using a phenomenological model proposed by Mott and Jones [6, 7]. According to this model the s–p electrons at the Fermi energy, E_F contributed by Al are responsible for carrying the current but are scattered into the final density of states $N(E_F)$. Consequently, the change in the resistivity is proportional to $N(E_F)$. They argued that as the aluminium concentration is increased, the s–p electrons of Al would fill the holes in the narrow d band of Fe and, consistent with band calculations, the total resistivity should increase. Beyond a critical Al concentration, the aluminium electrons would go into a free-electron-like conduction band and hence would lead to a decrease in resistivity. This simple picture is consistent with the electronic structure of free Fe and Al atoms. Since the energies of the Al 3p orbitals lie above the energy of the Fe 3d minority orbital, in an alloy of Fe and Al, the Al 3p electrons would spill into the holes in the Fe 3d orbital giving rise to a strong mixing of Fe 3d with Al 3p states. However, no calculations at the first principles level exist to determine (a) how the electronic structure of $Fe_{1-x}Al_x$ varies with x, or (b) to what extent the phenomenological model of Lilly *et al* [5] is valid.

There have been a few band structure calculations [8–14] that have attempted to understand the electronic structure of iron aluminides, but these are specific to the B2 phase with 50:50 composition of FeAl and the DO_3 phase of Fe_3Al. The band structure of FeAl is composed of a nearly free electron Al band crossing and mixing with a narrow Fe-derived d band. A proper understanding of the electronic structure of sub-stoichiometric $Fe_{1-x}Al_x$ would require band structure calculations involving a large unit cell as well as structural relaxation. Recently, a number of calculations using supercells containing up to 54 atoms have been carried out to probe the electronic structure of defects, namely those of vacancies and anti-site defects. Fu and co-workers [15] have calculated the defect formation energies in FeAl by using 16-atom and 32-atom supercells containing a single defect. More recently, Meyer and Fähnle [16] have studied the formation energies of atomic defects in the ordered compound B2-NiAl by combining *ab initio* electron theory and statistical mechanics and using a supercell containing 54 atoms. The effect of disorder on the onset of magnetism in Fe_xAl_{1-x} for $x = 0.4$, 0.5 and 0.6 was studied by Kulikov *et al* [17] by using the coherent potential approximation with the Korringa–Kohn–Rostoker method for the disordered case and the tight-binding linear muffin-tin orbital method for the intermetallic compounds. While band structure calculation using a large supercell is an ideal approach to study the electronic structure of defects in intermetallics, the quantitative accuracy of such calculations does depend on details of the calculations. This has been brought into focus by Wolverton and Zunger [18], who have shown that the earlier-predicted [19] Ni_7Al phase is unstable when calculations take into account spin polarization and full potential. The earlier calculation [19] was based on the local-density approximation

and linear muffin-tin orbitals within the atomic-sphere approximation (LMTO-ASA), rather than the full potential approach. We are not aware of any electronic band structure calculations on $Fe_{1-x}Al_x$ ($0 < x < 0.5$).

An alternative approach to treat such complex systems is to use a real-space method where the lack of symmetry and/or periodicity does not pose a potential problem. Such a method is based on a cluster approach where the bulk is modelled by a cluster of finite atoms. This approach has been used in the last 20 years for metallic and semi-conducting as well as insulating solids. In metallic systems where a defect is screened by the electrons, a cluster in which the probe site is dressed by atoms up to the second nearest neighbour shell has been found to be adequate [20]. Nevertheless, the cluster model has serious limitations. For a quantitative description, one would need to use a large cluster and demonstrate that the computed results indeed have converged with respect to cluster size. In view of the lack of information on the electronic structure of the $Fe_{1-x}Al_x$ ($0 < x < 0.5$) system, here we have attempted to provide a qualitative understanding of the electronic structure as a function of Al concentration considering a cluster of 15 atoms to model the interrmetallics.

Since Fe has a bcc lattice and the two ordered phases of iron aluminides, the B2 and the DO3, have cubic structures, we have assumed the cluster modelling $Fe_{1-x}Al_x$ to have bcc symmetry. Using the molecular orbital theory and the density functional formalism [21] with generalized gradient approximation [22] for the exchange-correlation potential, we have calculated the total energies, site-preference, atomic relaxation, electronic structure and magnetic properties of Fe_nAl_m ($n + m = 15$) clusters for various Al content. We show that our computed electronic structure is consistent with the phenomenological model of Lilly *et al* [5]. In addition, our calculations also yield interesting information on the magnetic behaviour of these alloys.

We briefly outline our theoretical procedure in section 2. The results are discussed in section 3 and a summary of our conclusions are given in section 4.

2. Theoretical procedure

The bulk phase of iron aluminide is modelled by a cluster of 15 Fe and Al atoms that mimic the bulk composition and bulk crystal structure. We begin with the Fe_{15} cluster assuming the structure of a bcc lattice where the body-centred atom is surrounded by two nearest neighbour shells of atoms (figure 1). We simulate increasing aluminium concentration by successively replacing Fe atoms with Al atoms. We have studied a range of clusters $Fe_{15-n}Al_n$ ($n = 0$, 1, 2, 3, 4, 5, 6, 7) that simulate Al concentration over a range $0 < x < 0.5$. In table 1 we denote which Fe atoms were replaced by Al atoms for a given composition, x. Note that for a given composition, it is necessary to examine more than one cluster as it is unclear which Fe atoms need to be replaced by Al atoms. We ultimately rely on the total energies to arrive at the preferred structure. For each composition we determine (i) the inter-atomic distance, (ii) the preferred site of Al in the cluster, (iii) the energy needed to replace successively Fe atoms with Al atoms, (iv) the electron density of states and (v) magnetic moments. These results are obtained through total energy calculations based on molecular orbital representation and density functional theory [21]. The exchange-correlation contribution to the potential is calculated using the generalized gradient approximation due to Becke *et al* [22]. The molecular orbitals of the clusters are expressed as a linear combination of atomic orbitals centred at individual atomic sites. We have used a double numeric basis set with polarization functions to express the atomic orbitals of Fe and Al. The basis set for Fe consisted of 3s, 3p, 3d and 4s orbitals along with a 4p polarization function, while the basis set for Al contained 3s and 3p orbitals with 3d-polarization functions. The core orbitals of Fe and Al were frozen. The

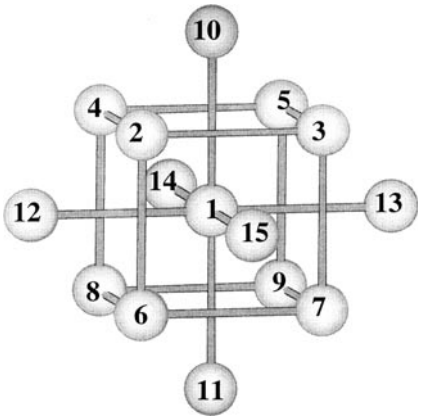

Figure 1. Geometry of Fe_{15} cluster having bulk bcc symmetry.

calculations were performed using the DMOL software [23]. Symmetries were employed in the calculations where applicable, but only for the relaxation of geometrical parameters. The symmetry, however, was broken while evaluating the Hamiltonian matrix elements.

Table 1. Location of Al atoms in $Fe_{15-n}Al_n$ ($n \leqslant 7$) cluster (see figure 1) and the corresponding binding energies.

n	Al concentration	Site location of Al atoms	Binding energy (eV)
1	6.7%	1	54.00
		12	53.92
		7	53.58
2	13.3%	1,12	52.91
		1,7	52.69
3	20.0%	1,12,13	51.93
		1,3,7	51.80
4	26.7%	1,12,13,10	50.79
		1,5,7,9	49.76
5	33.3%	1,10,11,12,13	49.27
		10,11,12,13,15	47.51
		1,3,5,7,9	45.79
6	40.0%	1,10,11,12,13,15	48.13
		10,11,12,13,14,15	47.85

In order to gain confidence in our calculations, we compare our results with earlier theories and available experiments. We begin this with a description of our results in atoms and dimers. The calculated ionization potentials of free Fe and Al atoms are respectively 7.65 eV and 6.02 eV, which compare well with the corresponding experimental values of 7.90 and 5.98 eV [24]. The calculated inter-atomic distances in Al_2 and Fe_2 are 2.51 Å and 2.07 Å, respectively. The increased bond length in Al_2 compared to that of Fe_2 is consistent with their ionic radii—1.43 Å for Al and 1.27 Å for Fe—and the bulk nearest-neighbour distance of 2.86 Å in Al and 2.49 Å in Fe [24]. Thus, when Al is substituted for Fe in $Fe_{1-x}Al_x$ one would expect an expansion of the lattice around Al sites. We will show later that this indeed is the case. In addition to the above calculations, we also evaluated the ground state of the Fe–Al dimer in order to compare its bond length with that obtained for the pure dimers of Fe and Al. The bond length of the Fe–Al dimer is

2.40 Å and is intermediate between the values obtained for the pure dimers of Fe and Al. The ground state revealed an antiferromagnetic coupling between Fe and Al with a net spin multiplicity of 4. The calculated moment on Fe is 3.5 μ_B while that on Al is -0.5 μ_B. We will show that this antiferromagnetic coupling between Fe and Al persists in larger clusters. The binding energy of the Fe–Al dimer (2.53 eV) is larger than that of Al_2 (1.76 eV). As we will see later, this determines the preferential site of Al in $Fe_{1-x}Al_x$.

We next discuss the properties of the Fe_{15} cluster and see to what extent it can mimic the properties of bulk Fe. First, we note that the nearest-neighbour distance in figure 1 is 2.38 Å, which is slightly less than the corresponding distance of 2.48 Å in bcc Fe. The binding energy in the Fe_{15} cluster is 3.64 eV/atom and is significantly less than the bulk cohesive energy of 4.28 eV. This is consistent with the general trend in free clusters, where the nearest neighbour distances approach the bulk value much more rapidly than the binding energies/atom [25].

The magnetic moment of the central Fe atom is 2.0 μ_B, which compares very well with the bulk magnetic moment of 2.2 μ_B. However, the magnetic moments of Fe atoms at the first and second shell are enhanced to 2.96 μ_B and 3.06 μ_B. This is a well-known phenomenon since atoms on the outer shells have low coordination number and reduced coordination leads to an enhancement in the magnetic moment [26]. To demonstrate this, we plot the total density of states of the Fe_{15} cluster as well as that derived from the central atom and the atom on the outermost shell in figure 2. Although the total density of states in Fe_{15} bears strong resemblance to the bulk density of states [27] (e.g., the width of the d-band, and the energy separation between the peaks agree well with the bulk data), the Fermi energy in the bulk density of states is shifted towards higher energy by about 1 eV. This disparity results from the larger splitting in the majority and minority spin states in the cluster model compared to that in the bulk band structure. As discussed above, the magnetic moments of the atoms in the outer shells of Fe_{15} are larger than the central site due to reduced coordination. Using the local spin density approximation, Lee *et al* [28] had calculated the magnetic moments at various Fe sites in the Fe_{15} cluster using a model of bulk bcc Fe. Their calculated average moment of 2.93 μ_B agrees well with our value of 2.94 μ_B.

We have modelled the stoichiometric FeAl phase by a cluster of Fe_8Al_7, which comes closest to the bulk composition. In this cluster the central atom and the atoms on the second shell in figure 1 consist of Al atoms while the atoms on the first shell are Fe atoms. In figure 2, we plot the total density of states of Fe_8Al_7. Also plotted in the figure are the density of states around the central and the outermost Al atoms. Ideally, in a band-structure calculation, the density of states around the central and the outermost atomic sites should be identical. While the features in figure 2 are similar for energies $\sim$3 eV below the Fermi energy, the densities of states for outer atoms near the Fermi energy are quantitatively different. This is due to the cluster size effect. Thus, while the cluster model may provide density of states qualitatively similar to those of the bulk, for a quantitative description one may have to go to very large clusters ($\sim$1000 atoms).

3. Results and discussion

In the following we discuss the atomic structure, energetics, electronic structure and magnetic properties of $Fe_{15-n}Al_n$ clusters.

3.1. Atomic structure

We begin with the results in the $Fe_{14}Al$ cluster. The energetically preferred structure is the one where the Al atom occupies the central site (see table 1 and figure 1). The distance between

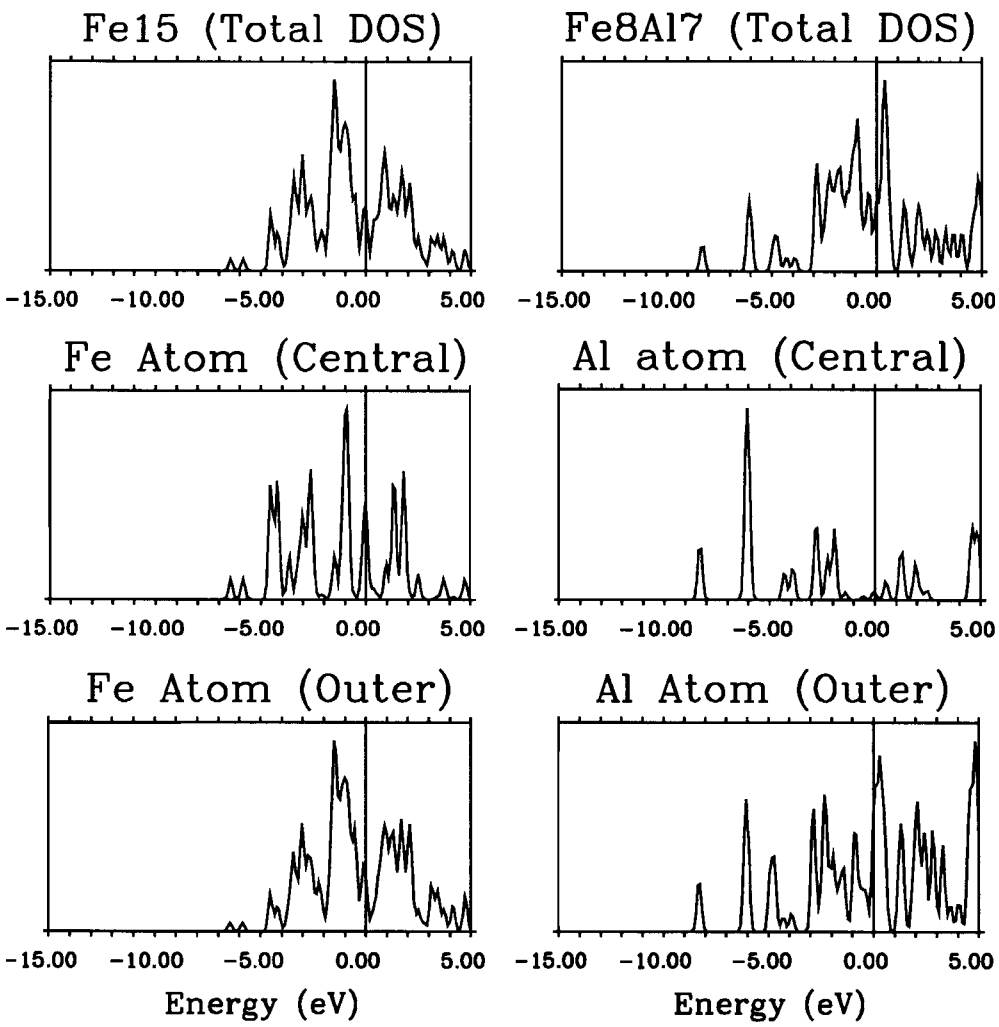

Figure 2. The total density of states of Fe_{15} and Fe_8Al_7 clusters. The corresponding contributions of the s, p, d states of the central Fe and the outermost Fe atoms for Fe_{15} and the corresponding s, p contributions of central and the outermost Al atoms to Fe_8Al_7 are also shown.

the central Al and the nearest Fe atoms is 2.45 Å, which is larger than the Fe–Fe distance of 2.38 Å in the Fe_{15} cluster. This is to be expected since, as mentioned before, the ionic radius of Al is larger than that of Fe. We note that the distance between Fe atoms in $Fe_{14}Al$ (2.38 Å) remains unchanged from that in Fe_{15}. This suggests that the perturbation caused by Al is effectively screened by the Fe atoms over a very small distance. The structures where Al atoms occupy the first or second shell are energetically less favourable. Since the Al atom occupying the central site has larger coordination of Fe atoms than that in the second or third shell, one could conclude that Al prefers to maximize its Fe coordination in an effort to lower the total energy of the system. As indicated earlier, this is evident from the behaviour in dimers.

There are two possible structures of $Fe_{13}Al_2$. Here, the two Al atoms can occupy the central site and a site on the second shell or they can occupy the central site and a site on the

first shell, thus becoming nearest neighbours. We find that the energetically preferred structure is the one where Al atoms do not like to be nearest neighbours. This again can be understood from the energetics of the dimers discussed earlier. Since the binding energy of the Fe–Al dimer is larger than that of Al_2, given a choice, Al can gain more energy by bonding to Fe atoms than by bonding to Al atoms. Thus in $Fe_{1-x}Al_x$ alloys where the concentration of Al is small, Al will be in a solid solution phase as opposed to a segregated phase. The Al–Fe (2.49 Å) and the Fe–Fe (2.39 Å) distances again remain similar to that in $Fe_{14}Al$.

In the $Fe_{12}Al_3$ cluster, the preferred structure has one Al atom at the centre while the other two are on the outermost shell farthest from each other. The Al–Fe and Fe–Fe distances again remain relatively unchanged from earlier structures. In $Fe_{11}Al_4$, one Al atom remains at the central site while the other three spread out on the outer shell so as to minimize their proximity to each other. A similar trend continues in $Fe_{10}Al_5$. Once again the Al–Fe (2.49 Å) and Fe–Fe (2.36 Å) distances remain very similar to previous clusters irrespective of Al content. In the Fe_9Al_6 cluster one would have expected the six Al atoms to occupy the sites on the third shell, as this would be a very symmetric structure. The contrary is the case. The preferred structure of Fe_9Al_6 has one Al atom at the central site while the rest occupy the sites on the third shell. Finally in the Fe_8Al_7 cluster, the central site and all of the third shell sites are occupied by Al. Substituting Al on the first shell will put two Al atoms into nearest-neighbour configuration, which as we have seen before, is energetically unfavourable.

3.2. Energetics

The energetics of $Fe_{15-n}Al_n$ clusters are analysed by calculating the binding energies, i.e. the energy necessary to dissociate the clusters into individual atoms as well as the energy cost to successively replace one Fe atom by an Al atom. The cohesive energy of Fe (4.28 eV) is larger than that of Al (3.39 eV). Thus, it would cost energy to replace an Fe atom by an Al atom. To examine how this energy cost evolves with Al concentration, we calculate

$$\Delta E_n = [E(\mathrm{Fe}_{15-n}\mathrm{Al}_n) - E(\mathrm{Fe}_{15})]/n \tag{1}$$

where $E(\mathrm{Fe}_{15-n}\mathrm{Al}_n)$ is the total energy of the $Fe_{15-n}Al_n$ cluster containing n Al atoms. We plot ΔE_n as a function of n in figure 3(a). As expected the energy increases monotonically with Al concentration and would reach an asymptotic value corresponding to the difference between the binding energy/atom of the Fe_{15} and Al_{15} clusters confined to the structure in figure 1.

The binding energy/atom of the $Fe_{15-n}Al_n$ cluster, on the other hand, is defined as

$$E_\mathrm{b} = -[E(\mathrm{Fe}_{15-n}\mathrm{Al}_n) - nE(\mathrm{Al}) - (15-n)E(\mathrm{Fe})]/15. \tag{2}$$

These are plotted in figure 3(b) as a function of n. Note that E_b decreases almost linearly as each Fe atom is successively replaced by an Al atom.

In order to achieve a qualitative understanding of these energetics in terms of the bulk cohesive energies of Fe and Al, we can analyse the binding energies of the cluster using a phenomenological model. Assuming a crude model where the binding energy/atom in $Fe_{15-n}Al_n$ scales with the cohesive energy of the individual atoms, one can approximately express the binding energy/atom $Fe_{15-n}Al_n$ as

$$E'_\mathrm{b} = [(15-n)E_\mathrm{c}(\mathrm{Fe}) + nE_\mathrm{c}(\mathrm{Al})]/n \tag{3}$$

where E_c is the cohesive energy of the respective metals (4.28 eV for Fe and 3.39 eV for Al). Using these results, we plot E'_b as a function of n in figure 3(b). Note that E_b and E'_b yield the same picture except a constant energy difference that mostly results from the finite cluster size effect. This comparison further illustrates that meaningful insight into the properties of iron aluminides can be obtained from a finite size cluster model.

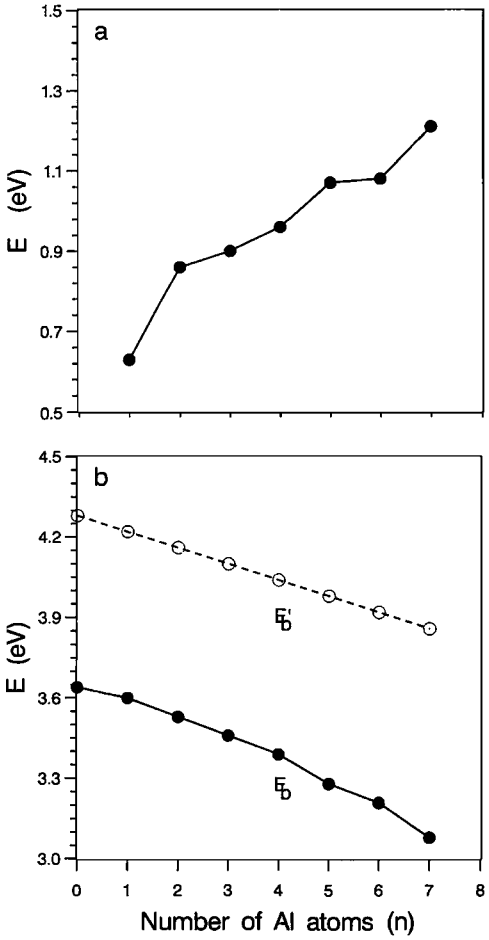

Figure 3. (a) The energy cost in successively replacing an Fe atom by an Al atom (equation (1)), (b) the binding energy/atom, E_b (equation (2)) and the phenomenological binding energy/atom, E'_b (equation (3)) plotted as a function of Al content.

3.3. Electronic structure

We now discuss the evolution of the electronic structure with increasing concentrations of Al. In figure 4 we show the total density of states for $Fe_{15-n}Al_n$ for $n = 0$, 1, 4, 5, 6 and 7. We have chosen the clusters that yield the lowest energy for each value of n (see table 1 and figure 1). These compositions mimic various representative values of x, i.e. at $x = 0$, 0.07, 0.27, 0.33, 0.40 and 0.47 in $Fe_{1-x}Al_x$ alloys. The position of the Fermi energy is defined as the zero of energy. Several interesting features of the total density of states (DOS) at various Al contents can be noted. At low Al content ($n = 1$), the DOSs are marked by several distinct peaks that resemble those in Fe_{15}. The DOS is progressively modified (broadening of the band near the Fermi energy) with increasing concentration of Al, and at $x = 0.47$ (Fe_8Al_7) we notice significant differences compared to the original features at $x = 0$. The density of states at E_F increases gradually with increasing Al content. It is also observed that the energy gap at the Fermi level decreases with increasing Al content resulting in a sharp peak of the density of states, just above the Fermi energy at $x \geqslant 0.33$.

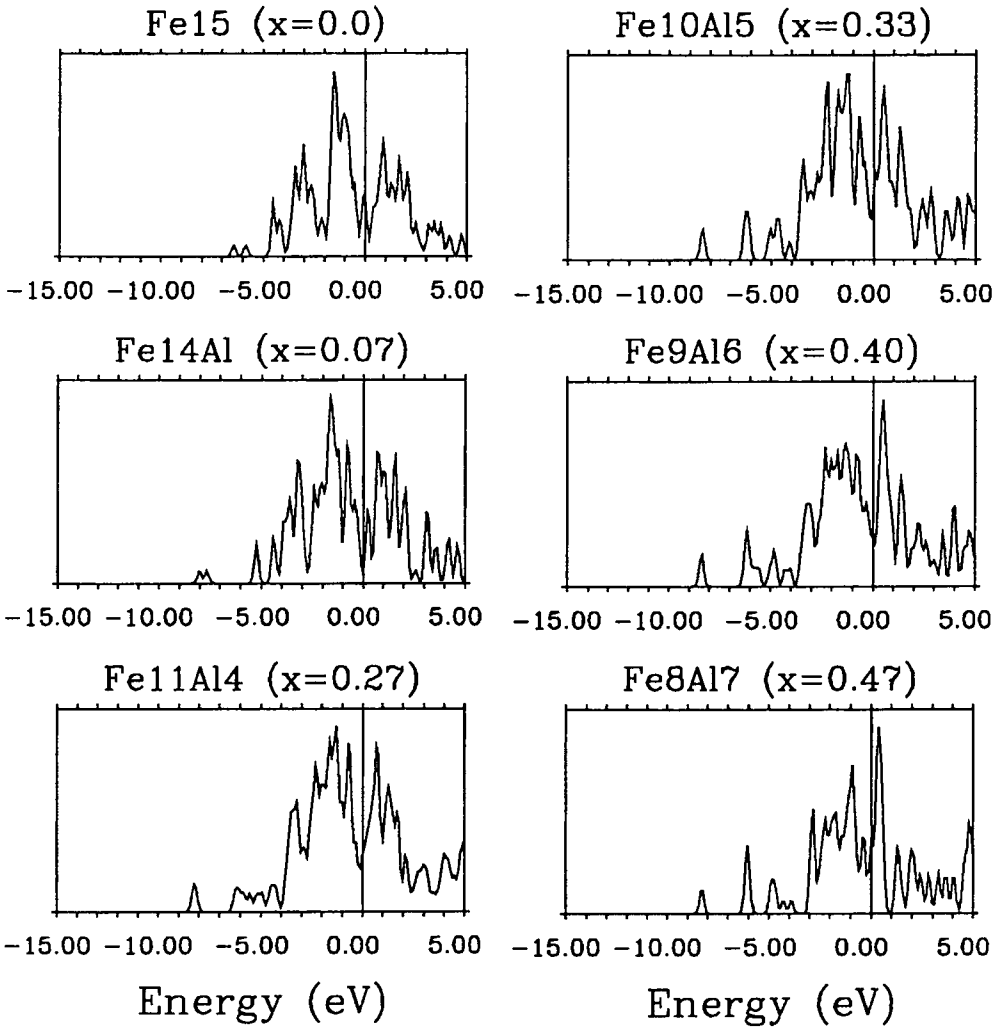

Figure 4. The total density of states in $Fe_{15-n}Al_n$ corresponding to (a) $n = 0$, (b) $n = 1$, (c) $n = 4$, (d) $n = 5$, (e) $n = 6$ and (f) $n = 7$.

At $x = 0$, i.e. or pure Fe_{15}, as indicated earlier, all the significant features of the bulk DOS are present. The Fermi level lies in the d manifold and in the steep minimum separating the two d peaks of the majority and minority carriers. At $x = 0.07$ ($Fe_{14}Al_1$), the additional features at energies beyond the Fermi energy are due to the p states of Al. At $x = 0.27$ ($Fe_{11}Al_4$), note that the lowest occupied band ($\sim$8 eV) has an Al 3s character. Following this, we observe a strong mixing effect of the Al p and Fe d states reflecting a modified density of states. The lowest unoccupied peak, now consisting of a strong p–d mixture, shifts closer to the Fermi level. This feature also implies a reduction in the overall exchange splitting between the majority and minority bands. These features progress with further increase of Al content and at $x = 0.40$ (Fe_9Al_6), we notice that the lowest unoccupied peak in the density of states becomes more dominant in Al 3p and shifts very close to Fermi energy. Finally, at $x = 0.47$ (Fe_8Al_7), the conduction band is mainly composed of strongly mixed Al p and Fe d levels. To

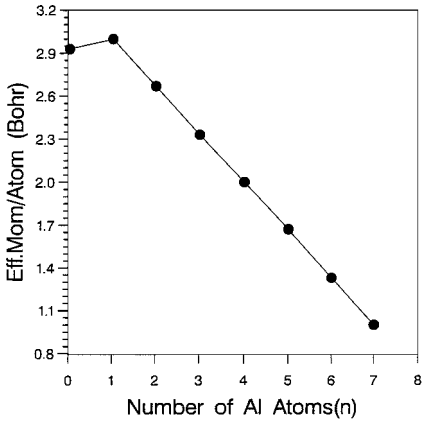

Figure 5. Average magnetic moment/atom as a function of Al content, n in the $Fe_{15-n}Al_n$ cluster.

demonstrate this more clearly, we see from figure 2 that the local density of states at the Fe sites arises from the 3d states and the 3p states from the outermost Al atoms.

It is worth pointing out that the Fermi level in stoichiometric FeAl, according to band structure studies [14, 15] lies in the Fe–Al bonding state region. This is consistent with our result for Fe_8Al_7 (figure 4(f)), that is closest to the stoichiometric composition. This further validates the use of cluster model as a qualitative tool for studying electronic structure.

3.4. Magnetic properties

We now discuss the magnetic structure of these $Fe_{15-n}Al_n$ clusters. As mentioned earlier, the coupling between the Fe and Al moments is antiferromagnetic. Although bulk of the moments are carried by Fe atoms, the Al atoms carry a small moment whose magnitude remains around 0.2 μ_B in all the clusters studied. Irrespective of the Al concentration, the moments at all Fe sites are parallel, as is the case with moments at all Al sites. However, the moments between Fe and Al are always antiferromagnetically coupled. This is in agreement with the original experiments of Arrot and Sato [29].

The magnitude of the magnetic moments at Fe sites in $Fe_{15-n}Al_n$ clusters varies as a function of Al concentration gradually decreasing with increasing Al content. One could understand this decrease as due to the constant increase of Fe 3d and Al 3p mixing accompanied by an increased delocalization of the d electrons participating in the strong bonding with Al. At this point, it should also be noted that an increase of Fe–Al coordination means a decreasing coordination of its own kind for Fe, which results in two important effects. The ferromagnetic coupling between Fe atoms is weakened due to the reduction of the coordination number of like neighbours as well as an increasing inter-atomic distance between them. Secondly, an increase of the Al coordination keeps the antiferromagnetic order of Fe–Al, while gradually quenching the moment on Fe.

To get further insight into the magnetic behaviour of iron aluminides, we plot in figure 5 the average magnetic moment/atom (=total magnetic moment (μ_B)/15) as a function of Al content of the clusters. We note that the average moment decreases linearly with Al concentration and would certainly vanish at concentrations where Al atoms would outnumber Fe atoms. This is consistent with the phase diagram where $FeAl_2$ and Fe_2Al_5 are known to be paramagnetic.

4. Conclusions

In summary, we have performed first principles calculations of the electronic structure and magnetic properties of $Fe_{15-n}Al_n$ clusters for various Al content by assuming the clusters to have the bcc structure of bulk Fe. The preferred site of Al as well as atomic relaxation around Al sites are calculated and can be qualitatively understood from the properties of constituent atoms and their dimers. The electronic densities of states near the Fermi energy are dominated by Fe 3d states in the Fe-rich phase of the alloy. As aluminium concentration increases, the holes in the Fe d band begin to fill and for $x > 0.3$, the density of states at the Fermi energy has a significant Al 3p character. This continuous change in the electronic structure brought about by the mixing of the Fe 3d and Al 3p is consistent with the observed anomaly in the electrical resistivity of $Fe_{1-x}Al_x$ where the resistivity rises for $0 < x < 0.3$ and decreases for $x > 0.3$. The magnetic behaviour of these clusters with increasing Al concentration is also interesting. Increasing concentration of Al atoms not only quenches the moment on Fe atoms, but also drives them farther apart due to their relatively large atomic sizes. Further, the exchange coupling between Fe and Al remains antiferromagnetic consistent with the early experimental measurements.

References

[1] Liu C T, George E P, Maziasz P J and Schneibel J H 1998 *Mater. Sci. Eng.* A **258** 84
[2] McKanney C G, Devan J H, Tortorelli P F and Sikka V K 1991 *J. Mater. Res.* **6** 695
[3] Deevi S C and Sikka V K 1996 *Intermetallics* **4** 357
[4] Deevi S C, Sikka V K and Liu C T 1997 *Prog. Mater. Sci.* **42** 177
[5] Lilly A C, Deevi S C and Gibbs Z P 1998 *Mater. Sci. Eng.* A **258** 42
[6] Mott N F and Jones H 1936 *The Properties of Metals and Alloys* (Oxford: Clarendon), reprinted 1958 (New York: Dover)
[7] Mott N F and Stevens K W H 1957 *Phil. Mag.* **2** 1364
[8] Nordheim L W 1931 *I. Ann. Phys., Lpz.* **9** 641
[9] Okochi M 1975 *J. Phys. Soc. Japan* **39** 367
[10] Homadinger G, Marksteiner G, Konig W and Weinberger P 1987 *Z. Phys. Condens. Matter* **67** 517
Caskey G R, Franz J M and Sellmyers D J 1973 *J. Phys. Chem. Solids* **34** 1179
[11] Koch J, Stefanou N and Koenig C 1986 *Phys. Rev.* B **33** 5319
[12] Botton G A, Guo G Y, Temmerman W M and Humphreys C J 1996 *Phys. Rev.* B **54** 1682
[13] Singh D 1994 *Intermetallic Compounds* vol 1, ed J H Westbrok and R L Fleischer (Chichester: Wiley) p 127
[14] Eibler R and Neckel A 1980 *J. Phys. F: Met. Phys.* **10** 2179
[15] Fu C L, Ye Y Y, Yoo M H and Ho K M 1993 *Phys. Rev.* B **48** 6712
[16] Meyer B and Fahnle M 1999 *Phys. Rev.* B **59** 6072
[17] Kulikov N I, Postnikov A V, Borstel G and Braun J 1999 *Phys. Rev.* B **59** 6824
[18] Wolverton C and Zunger A 1999 *Phys. Rev.* B **59** 12165
[19] Lu Z W, Wei S H, Zunger A, Frota-Pessoa S and Ferreira L G 1991 *Phys. Rev.* B **44** 512
[20] Press M, Liu F, Khanna S N and Jena P 1989 *Phys. Rev.* B **40** 399
[21] Kohn W and Sham L J 1965 *Phys. Rev.* **140** A1133
[22] Becke A D 1988 *Phys. Rev.* A **38** 3098
Becke A D 1988 *J. Chem. Phys.* **88** 2547
Perdew J P *et al* 1992 *Phys. Rev.* B **46** 6671
[23] DMOL Code version 950 (San Diego: Molecular Simulations)
[24] Kittel C 1996 *Introduction to Solid State Physics* 7th edn (New York: Wiley)
[25] Nayak S K, Khanna S N, Rao B K and Jena P 1997 *J. Phys. Chem.* A **101** 1072
[26] Liu F, Khanna S N and Jena P 1991 *Phys. Rev.* B **43** 8179
[27] Moruzzi V L, Janak J F and Williams A R 1978 *Calculated Electronic Properties of Metals* (New York: Pergamon)
[28] Lee K Y, Callaway J, Kwong K, Tang R Q and Zhegler A 1985 *Phys. Rev.* B **31** 1796
[29] Arrott A and Sato H 1959 *Phys. Rev.* **114** 1920
Sato H and Arrott A 1959 *Phys. Rev.* 1427